1521-0103/358/3/580–587$25.00
THE JOURNAL OF PHARMACOLOGY AND EXPERIMENTAL THERAPEUTICS

http://dx.doi.org/10.1124/jpet.116.234948
J Pharmacol Exp Ther 358:580–587, September 2016

Two Affinity Sites of the Cannabinoid Subtype 2 Receptor Identified by a Novel Homogeneous Binding Assay[S]

Eva Martínez-Pinilla, Obdulia Rabal, Irene Reyes-Resina, Marta Zamarbide, Gemma Navarro, Juan A. Sánchez-Arias, Irene de Miguel, José L. Lanciego, Julen Oyarzabal, and Rafael Franco

Neurosciences Division (E.M.-P., M.Z., J.L.L.) and Small Molecule Discovery Platform, Molecular Therapeutics Program (O.R., J.A.S.-A., I.d.M., J.O.), Centre for Applied Medical Research, University of Navarra, Pamplona, Spain; Instituto de Neurociencias del Principado de Asturias, Departamento de Morfología y Biología Celular, Facultad de Medicina, Universidad de Oviedo, Asturias, Spain (E.M.-P.); Departament de Bioquímica i Biología Molecular, Facultat de Biología,. Universitat de Barcelona, Barcelona, Spain (I.R.-R., G.N., R.F.); Centro de Investigación Biomédica en Red Enfermedades Neurodegenerativas, Madrid, Spain (I.R.-R., G.N., J.L.L., R.F.); Instituto de Investigaciones Sanitarias de Navarra, Pamplona, Spain (J.L.L.); and Institut de Biomedicina de la Universitat de Barcelona, Barcelona, Spain (R.F.)

Received May 5, 2016; accepted June 27, 2016

ABSTRACT

Endocannabinoids act on G protein–coupled receptors that are considered potential targets for a variety of diseases. There are two different cannabinoid receptor types: ligands for cannabinoid type 2 receptors (CB_2Rs) show more promise than those for cannabinoid type 1 receptors (CB_1Rs) because they lack psychotropic actions. However, the complex pharmacology of these receptors, coupled with the lipophilic nature of ligands, is delaying the translational success of medications targeting the endocannabinoid system. We here report the discovery and synthesis of a fluorophore-conjugated CB_2R-selective compound, CM-157 (3-[[4-[2-*tert*-butyl-1-(tetrahydropyran-4-ylmethyl)benzimidazol-5-yl]sulfonyl-2-pyridyl]oxy]propan-1-amine), which was useful for pharmacological characterization of CB_2R by using a time-resolved fluorescence resonance energy transfer assay. This methodology does not require radiolabeled compounds and may be undertaken in homogeneous conditions and in living cells (i.e., without the need to isolate receptor-containing membranes). The affinity of the labeled compound was similar to that of the unlabeled molecule. Time-resolved fluorescence resonance energy transfer assays disclosed a previously unreported second affinity site and showed conformational changes in CB_2R forming receptor heteromers with G protein–coupled receptor GPR55, a receptor for l-α-lysophosphatidylinositol. The populations displaying subnanomolar and nanomolar affinities were undisclosed in competitive assays using a well known cannabinoid receptor ligand, AM630 (1-[2-(morpholin-4-yl)ethyl]-2-methyl-3-(4-methoxybenzoyl)-6-iodoindole), and TH-chrysenediol, not previously tested on binding to cannabinoid receptors. Variations in binding parameters upon formation of dimers with GPR55 may reflect decreases in binding sites or alterations of the quaternary structure of the macromolecular G protein–coupled receptor complexes. In summary, the homogeneous binding assay described here may serve to better characterize agonist binding to CB_2R and to identify specific properties of CB_2R on living cells.

Introduction

Endocannabinoids are autocrine and paracrine regulators acting via two receptors: namely, CB_1 and CB_2. These cannabinoid receptors belong to the superfamily of G protein–coupled receptors (GPCRs). When they are activated by the endogenous agonists anandamide or 2-Arachidonoylglycerol, by the main psychoactive component of marijuana, or by synthetic cannabinoids, they couple to G_i and mediate decreases of intracellular cAMP levels while engaging mitogen-activated protein kinase pathways (Campillo and Páez, 2009; Atwood et al., 2012).

Cannabinoid receptors have been considered potential targets for a variety of diseases. Pharmaceutical developments led to the first-in-class, weight-reducing molecule

This research was supported by the University of Navarra Foundation for Applied Medical Research [Intramural Funds], the Spanish Ministry of Economy and Competitiveness [Grants SAF212-039875-C02-01 and BFU2012-37907; Grants PTQ-11-04781 and PTQ-11-04782 from Inncorpora-Torres Quevedo funds], and the Fundació La Marató de TV3 [Grants 20141330 and 20141331].
E.M.-P., O.R., J.L.L., J.O., and R.F. contributed equally to this work.
dx.doi.org/10.1124/jpet.116.234948.
[S] This article has supplemental material available at jpet.aspetjournals.org.

ABBREVIATIONS: AM630, 1-[2-(morpholin-4-yl)ethyl]-2-methyl-3-(4-methoxybenzoyl)-6-iodoindole; CB_1R, cannabinoid subtype 1 receptor; CB_2R, cannabinoid subtype 2 receptor; CM-139, 4-[2-*tert*-butyl-5-[(2-fluoro-4-pyridyl)sulfonyl]benzimidazol-1-yl]butan-1-amine; CM-157, 3-[[4-[2-*tert*-butyl-1-(tetrahydropyran-4-ylmethyl)benzimidazol-5-yl]sulfonyl-2-pyridyl]oxy]propan-1-amine; CP55940, (−)-*cis*-3-[2-hydroxy-4-(1,1-dimethylheptyl)phenyl]-*trans*-4-(3-hydroxypropyl)cyclohexanol; FRET, fluorescence resonance energy transfer; GPCR, G protein–coupled-receptor; HEK, human embryonic kidney; HTRF, homogeneous time-resolved fluorescence; ML056, (*R*)-3-amino-4-(3-hexylphenylamino)-4-oxobutylphosphonic acid; SR144528, 5-(4-chloro-3-methylphenyl)-1-[(4-methylphenyl)methyl]-*N*-[(1*S*,2*S*,4*R*)-1,3,3-trimethylbicyclo[2.2.1]hept-2-yl]-1*H*-pyrazole-3-carboxamide; TLB, Tag-lite labeling medium; WIN55212-2 [(11*R*)-2-methyl-11-[(morpholin-4-yl)methyl]-3-(naphthalene-1-carbonyl)-9-oxa-1-azatricyclo[6.3.1.$0^{4,12}$]dodeca-2, 4(12),5,7-tetraene.

rimonabant, which acted as a cannabinoid type 1 receptor (CB_1Rs) antagonist (Carai et al., 2006). Unfortunately, there were cases of suicide among individuals treated with rimonabant, and regulatory agencies thus withdrew the drug from the market (Sam et al., 2011). Cannabinoid subtype 2 receptors (CB_2Rs) are now considered better pharmacological targets than CB_1Rs because CB_2R-selective compounds have not the psychotropic risks derived from activating or blocking CB_1R in the central nervous system. CB_2R agonists are being assayed for pain (Zhang et al., 2013), osteoporosis (Idris, 2010; Sun et al., 2015), neuroprotection (Malek et al., 2015; Savonenko et al., 2015), and immune-related diseases (Leleu-Chavain et al., 2013). Thus far, the translational results have been disappointing. Multiple circumstances affect the negative results obtained by using CB_2R agonists (reviewed in Atwood et al., 2012). On one hand, the CB_2R knockout mouse does not present gross morphologic alterations with respect to wild-type animals but has served to link the receptor to a wide range of physiologic processes and pathophysiological conditions (Buckley, 2008). On the other hand, data in the literature clearly show that CB_2R pharmacology is complex.

Like many other class A, rhodopsin-like GPCRs, cannabinoid receptors may form heteromers, which are receptor complexes with differential features compared with those of single-component units (Ferré et al., 2009). CB_1Rs may form heteromeric complexes with CB_2 (Callén et al., 2012), L-α-lysophosphatidylinositol (Martínez-Pinilla et al., 2014), δ-opioid (Bushlin et al., 2012), μ-opioid (Rios et al., 2006; Hojo et al., 2008), orexin-1 (Ellis et al., 2006), and dopamine D_2 and adenosine A_{2A} (Navarro et al., 2008; Przybyla and Watts, 2010) receptors. To date, apart from CB_1R (Callén et al., 2012), only G protein-coupled receptor GPR55 (Balenga et al., 2014) has been described as a heteromeric partner of CB_2R.

Homogeneous time-resolved fluorescence (HTRF) is an increasingly used technique performed in living cells. It detects ligand binding to receptors tagged with SNAP (see the *Materials and Methods*). Its advantages include the possibility of conducting homogeneous assays in which radiolabeled compounds are not required. This investigation aimed to synthesize a high-affinity and CB_2R-selective ligand that could be used in binding assays using HTRF. The novel compound was used to characterize the in vivo binding of cannabinoid ligands to CB_2R and served to disclose two affinity states of this receptor.

Materials and Methods

Materials and Reagents. High-performance liquid chromatography–grade acetonitrile was purchased from Merck (Darmstadt, Germany) and liquid chromatography/mass spectrometry–grade methanol was from Scharlau Chemie (Barcelona, Spain). Liquid chromatography/mass spectrometry–grade formic acid and acetic acid were provided by Sigma-Aldrich (St. Louis, MO). 3′,5′-cGMP and 3′,5′-cAMP were obtained from Carbosynth (Berkshire, UK). The stable isotope-labeled sildenafil-d_3, ^{13}C,$^{15}N_2$-cGMP, and $^{13}C_5$-cAMP, used as internal standards, were supplied by Toronto Research Chemicals (Toronto, ON, Canada). Ultrapure water (18 MΩcm) was generated using a Milli-Q system (Millipore, Bedford, MA). Other chemicals and solvents (unless otherwise specified) were of analytical or high-performance liquid chromatography grade from Panreac Química (Madrid, Spain) or Sigma-Aldrich. C-18 Light Sep-Pak cartridges were obtained from Waters (Milford, MA) and were preconditioned, sequentially, with ethanol (5 ml) and water (5 ml).

For nonradioactive binding assays, Tag-lite labeling medium (TLB) was obtained from Cisbio Bioassays (LABMED; Codolet, France). The Tb derivative of O_6-benzylguanine was synthesized by Cisbio Bioassays and is commercialized as SNAP-Lumi4-Tb (SSNPTBC; Cisbio Assays). CB_2R agonists CM-157 (3-[[4-[2-*tert*-butyl-1-(tetrahydropyran-4-ylmethyl)-benzimidazol-5-yl]sulfonyl-2-pyridyl]oxy]propan-1-amine) and CM-139 (4-[2-*tert*-butyl-5-[(2-fluoro-4-pyridyl)sulfonyl]benzimidazol-1-yl]butan-1-amine), conjugated to red-naltrexone fluorescent probes (red CB_2R ligands) were developed by Cisbio Bioassays. The various agonists used for competition assays, AM630 (1-[2-(morpholin-4-yl)ethyl]-2-methyl-3-(4-methoxybenzoyl)-6-iodoindole) and TH-chrysenediol, were obtained from Tocris Bioscience (Bristol, UK). Stock solutions were prepared in dimethylsulfoxide. Aliquots of these stock solutions were kept frozen at −20°C until use. The plasmid encoding for the SNAP-tagged human CB_2R used for transient transfection was obtained from Cisbio Bioassays (PSNAP-CB2). White opaque 384-well plates were obtained from PerkinElmer (Wellesley, MA).

CB_2R Agonists: Selection of CM-157 and Design of CM-139. A total of 173 compounds and their pEC_{50} values against CB_2R were manually compiled from patents WO2006048754 and WO2008003665 (Kon-I et al., 2006; Gijsen et al., 2008). Then, we analyzed R-group patterns at each derivatization position of the central benzimidazole scaffold by using our in-house tool for exploring the biologically relevant chemical space (BRCS navigator; Rabal and Oyarzabal, 2012), which is especially suitable for competitive intelligence and patent analysis. Roughly, in this approach, each R-group is characterized by the chemical functionality of its attachment point to the central scaffold (a total of 14 classes) and by the chemical nature of the substitution pattern behind the attachment point (a total of 17 classes). As a summary of the analysis is as follows: at nitrogen 1 (N1), 140 of the 173 compounds bear an aliphatic heterocycle, more precisely a tetrahydropyrane ring (105 compounds). At carbon 2 (C2), aliphatic chains are mostly preferred (e.g., *tert*-butyl). Finally, at carbon 5 (C5), most R-groups are aromatic heterocycles (e.g., pyridine rings) bearing a single substitution that are attached to the scaffold by a sulphonamide moiety (Supplemental Fig. 1).

Taking into account the previously reported key chemical features to obtain optimal primary activity *versus* CB_2Rs as well as the plausible spatial orientation (confirmed by docking studies, below) for functional group (a primary amine) to label proposed molecules in just one synthetic step, we proposed and synthesized two molecules: CM-139 (novel designed compound) and CM-157 (molecule 131 in patent WO2008003665; Gijsen et al., 2008) (Fig. 1). Supplemental Schemes 1-4 describe the synthesis and characterization of CM-139 and CM-157. Then, these two molecules were labeled with red-naltrexone fluorescent probes by Cisbio Bioassays and became potential red CB_2R ligands.

Cell Line Cultures and Transfection. Human embryonic kidney (HEK)-293T cells were grown in Dulbecco's modified Eagle's medium supplemented with 2 mM L-glutamine, 1 mM sodium pyruvate, 100 U/ml penicillin/streptomycin, and 5% (v/v) heat-inactivated fetal bovine serum (all supplements were from Invitrogen, Paisley, Scotland, UK). Cells were maintained at 37°C in a 5% CO_2 humidified atmosphere and were passaged, with enzyme-free cell dissociation buffer (13151-014; Gibco/ Thermo Fisher Scientific, Waltham, MA), when they were 80%-90% confluent (i.e., approximately twice a week).

For fluorescent ligand-binding assays, HEK-293T cells grown in 25-cm^2 flasks were transiently transfected with the SNAP-CB_2R plasmid with or without GPR55 cDNA cloned in pcDNA3.1 by the Lipofectamine 2000 method (11668-019; Invitrogen/Thermo Fisher Scientific, Waltham, MA). When 60% confluence was reached, the cell medium was removed and replaced with 4 ml fresh medium. As a control, a transfection mix containing 8 μg plasmid, 20 μl Lipofectamine 2000, and 1 ml Opti-MEM without serum (51985-026; Gibco/ Thermo Fisher Scientific) final volume was incubated for 20 minutes at room temperature prior to being added to cells. The culture flask was incubated at 37°C under 5% CO_2 for 24 hours.

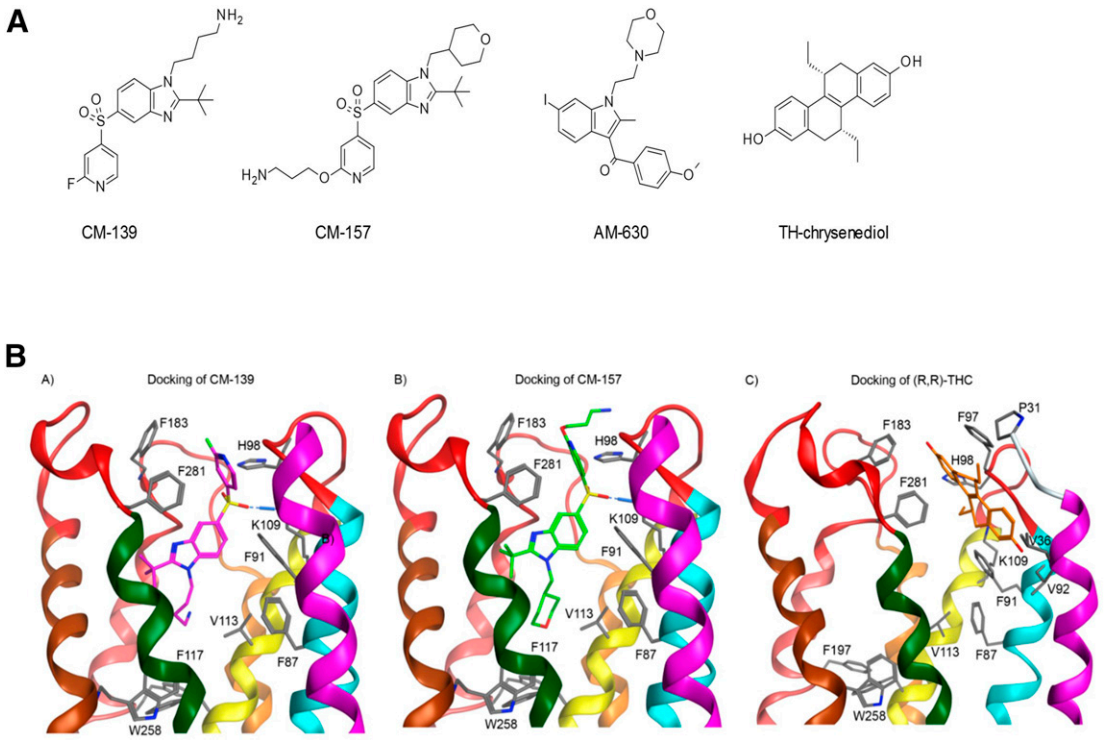

Fig. 1. (A) Chemical structure of compounds. (B) Docking of CM-139, CM-157, and TH-chrysenediol to the putative orthosteric site in CB_2Rs.

Covalent Labeling of Cells Expressing SNAP-Tagged CB_2R. The cell culture medium was removed from the 25-cm^2 flask and 100 nM SNAP-Lumi4-Tb, previously diluted in 3 ml TLB 1×, was added to the flask and incubated for 1 hour at 37°C under 5% CO_2 in a cell incubator. Afterward, cells were washed four times with 2 ml TLB 1× to remove the excess of SNAP-Lumi4-Tb, detached with enzyme-free cell dissociation buffer, centrifuged for 5 minutes at 1500 rpm, and collected in 1 ml TLB 1×.

Nonradioactive Homogeneous Binding Assays. Tag-lite-based binding assays (Fig. 2A) were performed 24 hours after transfection. Densities from 2500 to 3000 cells per well were used to carry out binding assays in suspension in white opaque 384-well plates.

Saturation binding experiments (Fig. 2B and C) were performed by incubating cells expressing Tb-labeled SNAP-CB_2R with increasing concentrations of the red CB_2R ligand (range, 0-300 nM final) in TLB 1×. For each concentration, nonspecific binding was determined by adding 100 μM unlabeled CM-157 or CM-139. Both fluorescent ligands and unlabeled compounds were diluted in TLB 1×. In the plates containing 10 μl labeled cells, 5 μl of 100 μM unlabeled CM-157, CM-139, or TLB 1× was added, followed by the addition of 5 μl of increasing concentrations of the red CB_2R ligand. Plates were incubated for 2 hours at room temperature before signal reading.

For the competition binding assay (Fig. 3A), the red CB_2R ligand and the compounds to be tested were diluted in TLB 1×. Cells were incubated with 20 nM or 100 nM red CB_2R ligand in the presence of increasing concentrations (range, 0-10 μM) of the competitor. In plates containing 10 μl labeled cells, 5 μl TLB 1× or 5 μl compound to be tested was added prior to the addition of 5 μl fluorescent ligand. Plates were then incubated for at least 2 hours at room temperature before signal detection.

Signal Detection and Data Analysis. The signal was detected using an EnVision microplate reader (PerkinElmer, Waltham, MA) equipped with a fluorescence resonance energy transfer (FRET) optic module allowing donor excitation at 337 nm and signal collection at both 665 and 620 nm. A frequency of 10 flashes per well was selected for the xenon flash lamp excitation. The signal was collected at both 665 and 620 nm using the following time-resolved settings: delay, 150 μs; and integration time, 500 μs. HTRF ratios were obtained by dividing the acceptor signal (665 nm) by the donor signal (620 nm) and multiplying this value by 10,000. The 10,000 multiplying factor was used solely for the purpose of easier data handling.

Data were then analyzed using Prism 6 software (GraphPad Software, Inc., San Diego, CA). K_D values of the fluorescent ligands were obtained from saturation curves of the specific binding. Specific binding was determined by subtracting the nonspecific HTRF ratio from the total HTRF ratio. K_D and B_{max} values in saturation experiments were calculated assuming one or two binding sites in monomeric receptors or, when indicated, receptor dimers. Unlike in radioligand binding assays, B_{max} values obtained from HTRF data do not reflect absolute values of receptor binding sites; they are, however, useful for comparison purposes. K_i values were determined from competitive binding experiments, according to the Cheng-Prusoff equation. Signal-to-background ratio calculations were performed by dividing the mean of the maximum value (μ_{max}) by that of the minimum value (μ_{min}) obtained from the sigmoid fits.

Results

Structure-Activity Relationships to Select a Fluorophore-Conjugated Ligand for HTRF Binding. Although there are a number of GPCRs for which the fluorescent ligand for HTRF is available, this is not the case for CB_2R. The attachment of the fluorophore was performed in two selective CB_2R ligands, CM-139 and CM-157 (Fig. 1A), with the purpose of exploring different potential binding modes. Both compounds share a benzimidazole core that is decorated at a different position with an alkyl amine to which the fluorophore is anchored. Using our in-house tool for patent analysis (Rabal and Oyarzabal, 2012), CM-157 was selected as the best candidate after analyzing 173 compounds from two patent applications (WO2006048754 and WO2008003665; Kon-I et al., 2006; Gijsen et al., 2008) claiming benzimidazoles as cannabinoid agonists. Briefly, the compound was selected

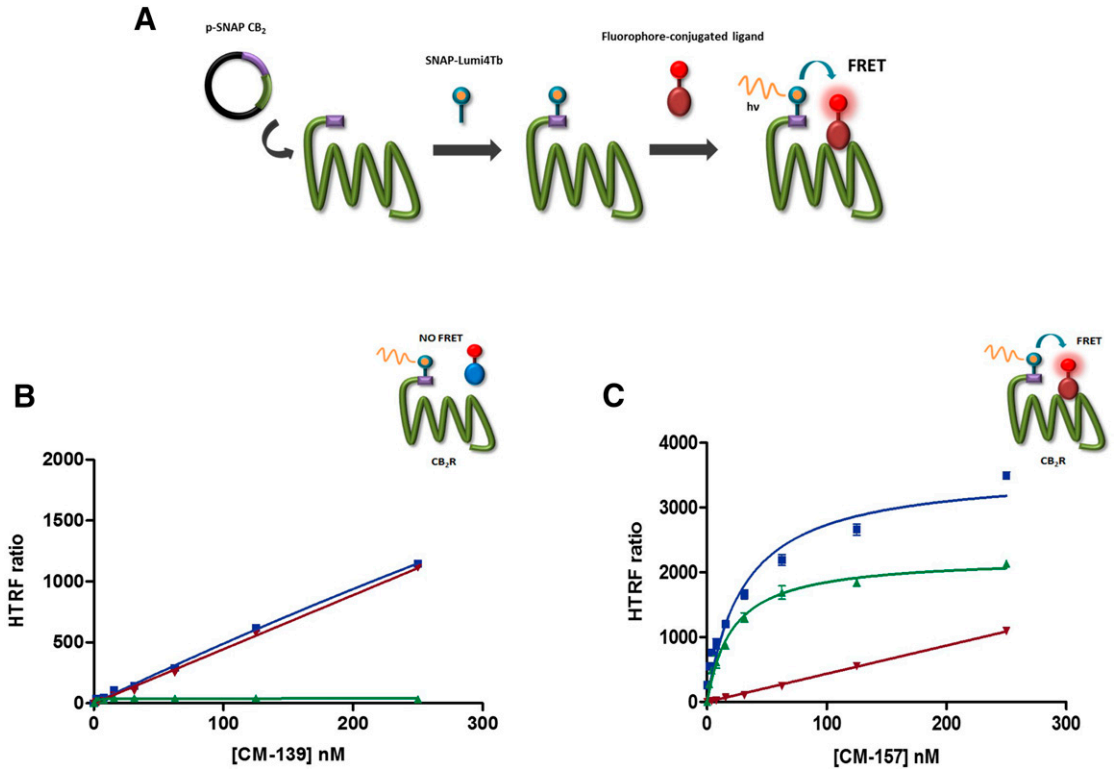

Fig. 2. Binding of CM-157 and CM-139 to Tb-labeled SNAP-CB_2R monitored by HTRF. (A) Scheme of the homogenous HTRF-based binding technique. The GPCR of interest fused at the N-terminal part with the SNAP-tagged enzyme is expressed at the cell surface. The GPCR–SNAP-tagged cells are subsequently labeled with SNAP-Lumi4-Tb through a covalent bond between the terbium donor and the reactive side of the SNAP enzyme. Upon binding of a fluorophore-conjugated ligand (FRET acceptor) on the donor-labeled SNAP-tagged/GPCR fusion protein, an HTRF signal from the sensitized acceptor can be detected since the energy transfer can occur only when the donor and the acceptor are in close proximity. (B) Saturation binding experiments of CM-139 on SNAP-CB_2R transiently transfected HEK-293T cells prelabeled with SNAP-Lumi4-Tb. The specific binding signal (triangles) was calculated by subtracting the nonspecific signal (inverted triangles) determined in the presence of 100 μM unlabeled CM-139 from the total binding signal (squares). A very low total binding signal overlaps with nonspecific signal. (C) Saturation binding experiments of CM-157 on SNAP-CB_2R-expressing cells gave a K_D of 21 $\pm$ 2 nM, determined by fitting to the one-site binding (hyperbola) equation. Values represent the mean $\pm$ S.E.M. of three independent experiments. The HTRF ratio was 665 nm acceptor signal/620 nm donor signal $\times$ 10,000.

on the basis of its potency as well as its representativeness of the most frequent substitution patterns of the R-groups at the different positions (N1, C2, and C5) of the scaffold sampled by these 173 compounds. In addition, based on the patent analysis, CM-139 was explicitly designed to include these preferred R-groups at the different positions of the benzimidazole core while enabling fluorophore derivatization at the nitrogen (N1) of the benzimidazole core. Thus, according to plausible binding modes, two potential spatial orientations to accommodate a solvent-exposed red dye (playing its functional role for energy transfer) while keeping primary activity were explored. One orientation should achieve obtaining a red CB_2 ligand to perform nonradioactive labeling of CB_2R and, likely, the second one should not be useful for such aim.

To our knowledge, there is currently no crystallographic information on CB_2R. To understand the common binding motives in these two compounds, a sphingosine 1-phosphate receptor–based homology model of CB_2R was built, and compounds were docked into the potential orthosteric ligand-binding pocket. As shown in Fig. 1B, the sulfonamide moiety of the two compounds would predictably establish a hydrogen bond with Lys^{109} (3.28), the equivalent residue to that in the CB_1R that is critical for recognition of several cannabinoids (Tao et al., 1999). To further validate our modeling methodology, we took advantage of the fact that one CB_2R cannabinoid ligand, CP55940 [(−)-*cis*-3-[2-hydroxy-4-(1,1-dimethylheptyl)phenyl]-*trans*-4-(3-hydroxypropyl)cyclohexanol], does not interact with Lys^{109} (Tao et al., 1999). In fact, our docking procedure showed that this residue is not involved in binding of CP55940 to CB_2R.

The *n*-butyl amine (in CM-139) and the tetrahydropyran (in CM-157) chains inserted into a large hydrophobic cavity formed by residues in transmembrane helices 3, 5, 6, and 7 are flanked by Val^{113} (3.32), Phe^{117} (3.36), and Trp^{258} (6.48). These chains superpose well with the phenyl acyl tail of the selective sphingosine-1-phosphate receptor 1 agonist, ML056 [(*R*)-3-amino-4-(3-hexylphenylamino)-4-oxobutylphosphonic acid], bound to the sphingosine 1-phosphate receptor. This receptor belongs to the same subfamily, A13, as cannabinoid receptors (data not shown). Finally, the pyridine ring of both compounds forms a π–π interaction with Phe^{281} (7.35), and *meta*- or *para*-substituents of the pyridine ring would point toward the extracellular loops of CB_2R. Thus, according to our proposed binding mode, derivatization of compound CM-139 at the *n*-butyl amine moiety would prevent its binding to CB_2R, whereas derivatization of compound CM-157 at the 3-methoxypropan-1-amine would extend into the extracellular domain of CB_2R. These two options to conjugate the fluorophore were further considered.

The two resulting fluorophore-labeled compounds were assayed using HEK-293T cells expressing SNAP-CB_2R covalently linked to the terbium time-resolved FRET donor (SNAP-Lumi4-Tb, see the *Materials and Methods*). Binding

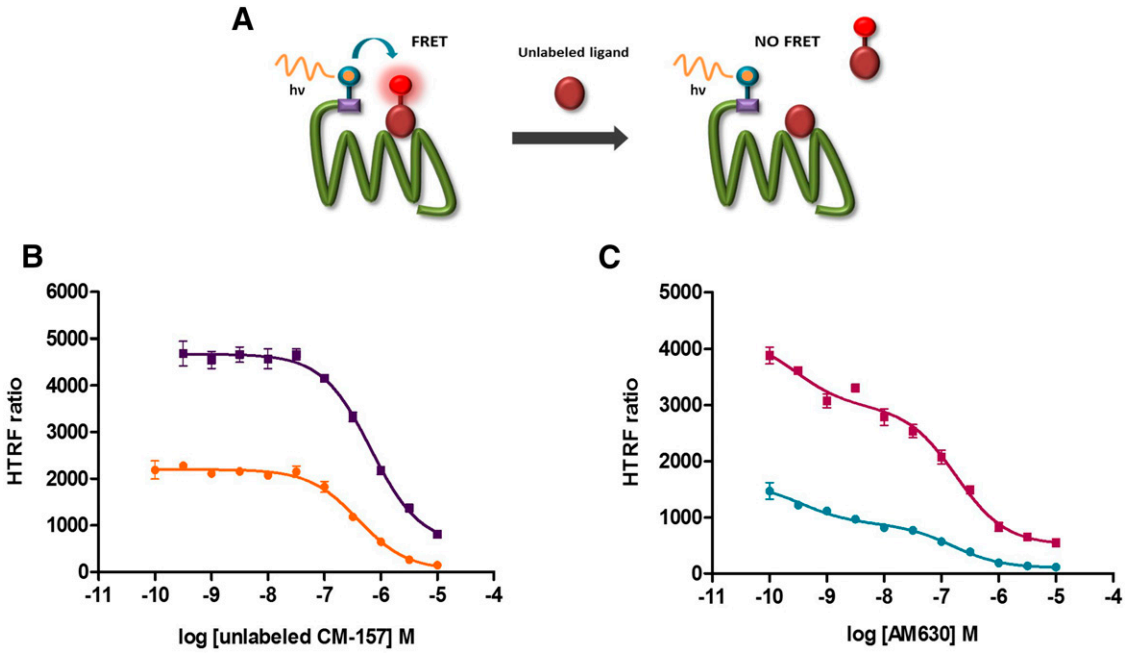

Fig. 3. Competition binding assays using CM-157 and AM630, a CB_2R antagonist/inverse agonist. (A) Scheme of the HTRF-based competitive binding assay. The unlabeled specific ligand competes for receptor binding site with the fluorophore-conjugated ligand, leading to a decrease in the HTRF signal detected. (B) Competition binding of 20 nM (circles) and 100 nM (squares) labeled CM-157 to SNAP-CB_2R with increasing concentrations of unlabeled CM-157 shows monophasic curves with K_i values of 233 nM and 153 nM, respectively. (C) Competition binding of the CB_2R antagonist/inverse agonist AM630 shows a clear biphasic curve. Data fitting to two affinity sites gives a K_{iHigh} of 0.2 nM and a K_{iLow} of 93 nM when competing with 20 nM labeled CM-157 (circles) and a K_{iHigh} of 0.07 nM and a K_{iLow} of 41 nM when competing with 100 nM labeled CM-157 (squares). Values represent the mean ± S.E.M. of three independent experiments. The HTRF ratio is 665 nm acceptor signal/620 nm donor signal × 10,000.

using fluorophore-labeled CM-139 was mainly nonspecific (Fig. 2B), whereas the specific binding using fluorophore-labeled CM-157 was notable and led to a saturable dose-response relationship (Fig. 2C). K_D values for labeled CM-157 obtained by saturation isotherms were in a range (19-35 nM) that fits with EC_{50} values for CB_2R agonism using WIN55212-2 [(11*R*)-2-methyl-11-[(morpholin-4-yl)methyl]-3-(naphthalene-1-carbonyl)-9-oxa-1-azatricyclo[6.3.1.$0^{4,12}$]-dodeca-2,4(12),5,7-tetraene] as reference compound (pEC_{50} = 7.8; Gijsen et al., 2008). Therefore, as we expected, dye labeling at the solvent-exposed area of selected ligands leads to energy transfer and the possibility of homogeneous binding and similar parameters as those obtained in radioactive assays. The synthesized reagent may be used in living cells for nonradioactive labeling of CB_2R with a performance similar to that of other ligand-GPCR systems for which the reagents for the Cisbio Taglite technology are commercially available.

One important advantage of the HTRF technique is that inhibition of the FRET signal due to competitive binding with unlabeled compounds can be used to identify and characterize new GPCR ligands. Therefore, competition experiments were performed in HEK-293T cells expressing SNAP-CB_2R covalently linked to the terbium donor, using two different concentrations (20 and 100 nM) of labeled CM-157 and increasing concentrations of unlabeled CM-157 (Fig. 3A). Curves were monophasic and the K_i value ranged from 153 to 233 nM (Fig. 3B). Overall, the data indicate the suitability of the CB_2R ligand for homogenous binding determination. To further check for similar characteristics of the binding site compared with radioligand binding, competition assays were performed using increasing concentrations of unlabeled AM630 and either 20 or 100 nM fluorescence-labeled CM-157. At any of the two concentrations of the labeled compound, competition curves were biphasic and, accordingly, data were fitted to two affinity sites. The affinity parameters ranged from 0.067 to 0.2 nM for K_{iHigh} and from 42 to 93 nM for K_{iLow} (Fig. 3C).

Binding to CB_2R in Living Cells Expressing CB_2R-GPR55 Heteromers. Class A GPCRs can form heteromers, and it is of great interest to know whether heteromerization affects the pharmacological characteristics of receptors. CB_2R may heteromerize with CB_1R (Callén et al., 2012) or with GPR55 (Balenga et al., 2014). Competition experiments were performed in HEK-293T cells coexpressing SNAP-CB_2R, covalently linked to the terbium donor, and GPR55, using labeled CM-157 (100 nM) and increasing concentrations of unlabeled CM-157 (Fig. 4A). Curves were monophasic (Fig. 4B) and showed a significant decrease in the maximum binding, in the presence of GPR55, without significant modification of the K_i value of the competitor CM-157. In a different experimental session, saturation curves using increasing concentrations of the labeled compound in cells coexpressing the two receptors had a 38% reduction in B_{max} compared with cells expressing CB_2R alone (Fig. 4C). This finding indicates that coexpression of the two receptors able to form receptor complexes modifies the number of binding sites or, more likely, the relative distance between the FRET donor and acceptor. Affinity was not significantly different (K_D = 25 and 58.5 for SNAP-CB_2R and SNAP-CB_2R/GPR55, respectively), although a tendency to lower K_D values was found in cells expressing only tagged CB_2R.

Identification of TH-chrysenediol Binding to CB_2R. Among a battery of compounds with diverse chemical structure, HTRF confirmed the absence of binding of noncannabinoid

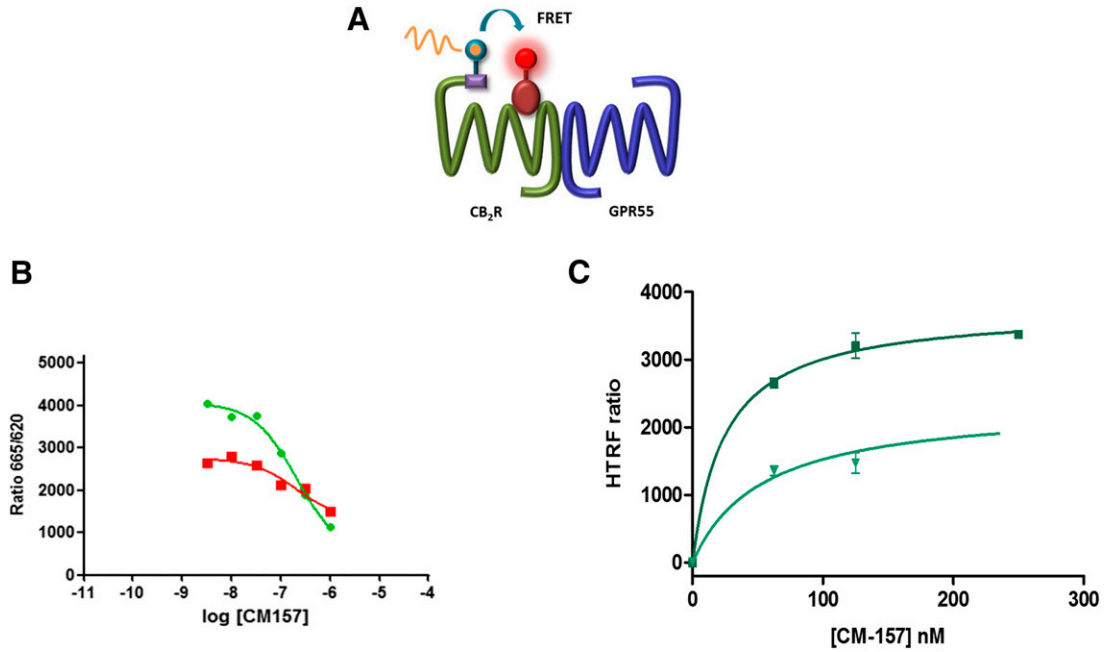

Fig. 4. Competition assays using CM-157 in cells expressing CB_2Rs and GPR55. (A) Scheme of the HTRF-based competitive binding assay in cells coexpressing two receptors: SNAP-CB_2R covalently linked to the terbium donor and GPR55. (B) Competition binding of 100 nM labeled CM-157 in HEK-293T cells expressing SNAP-CB_2R (circles) or SNAP-CB_2R/GPR55 (squares), with increasing concentrations of unlabeled CM-157, show monophasic curves. (C) Saturation binding experiments of CM-157 in HEK-293T cells transiently transfected with SNAP-CB_2R (squares) or SNAP-CB_2R/GPR55 (inverted triangles); data fitting to the one-site binding (hyperbola) equation gives a K_D of 25 ± 4 nM and a B_{max} of 3751 ± 110 and a K_D of 58.5 ± 45 nM and a B_{max} of 2327 ± 557, respectively. Specific binding was calculated by subtracting the nonspecific signal determined in the presence of 100 μM unlabeled CM-157 from the total binding signal. Values represent the mean ± S.E.M. of three independent experiments. The HTRF ratio is 665 nm acceptor signal/620 nm donor signal × 10,000.

compounds to tagged CB_2R with one exception, TH-chrysenediol. Interestingly, competition assays performed using 100 nM labeled CM-157 and increasing concentrations of TH-chrysenediol consistently led to a biphasic curve. Data fitting to two different affinity sites gave a K_{iHigh} of 13 pM and a K_{iLow} of 82 nM (Fig. 5A).

To obtain more insight on the nature of these biphasic competition curves, saturation experiments were performed in HEK-293T cells expressing SNAP-CB_2R and using increasing concentrations of fluorophore-conjugated CM-157 in the presence of 10 or 100 nM TH-chrysenediol (Fig. 5B). Interestingly, the Scatchard representation of the CM-157 binding isotherm was nonlinear and the data were adjusted to one affinity site, to two affinity sites, and to the two-state dimer model, which assumes that binding to CB_2R dimers occurs (see Table 1). In the absence of TH-chrysenediol, the maximal amount of receptors (B_{max}, B_{High} plus B_{Low}, or twice the number of dimers) was similar. When considering one or two affinity sites, the presence of 10 nM TH-chrysenediol decreased the affinity for CM-157 binding to CB_2R but not the maximum binding (B_{max} or B_{High} plus B_{Low}) (Table 1). The third fitting approach gave a qualitatively different result because the amount of receptors decreased, whereas the dissociation constants for binding to the two protomers in a

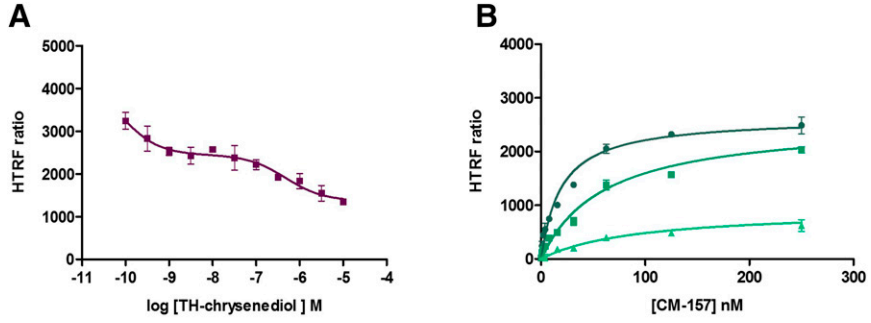

Fig. 5. Characterization of TH-chrysenediol binding to CB_2R. (A) Competition binding of 100 nM labeled CM-157 to SNAP-CB_2R with increasing concentrations of TH-chrysenediol shows a clear biphasic curve. Data fitting to two affinity sites gives a K_{iHigh} of 13 pM and a K_{iLow} of 82 nM. (B) Saturation binding experiments of CM-157 in HEK-293T cells transiently transfected with SNAP-CB_2R in the presence of 0 nM (circles), 10 nM (squares), or 100 nM (triangles) TH-chrysenediol. Specific binding signals were calculated by subtracting the nonspecific signal determined in the presence of 100 μM unlabeled CM-157 from the total binding signal. Values represent the mean ± S.E.M. of three independent experiments. The HTRF ratio is 665 nm acceptor signal/620 nm donor signal × 10,000.

TABLE 1
CM-157 binding parameters, in the absence and presence of TH-chrysenediol, calculated by different fitting protocols

Condition	One Site		Two Sites				Dimer		
	K_D	B_{max}	K_{DHigh}	K_{DLow}	B_{High}	B_{Low}	K_1	K_2	R_T[a]
	nM	*RU*	*nM*		*RU*		*nM*		*RU*
CM-157	19	2634	1.8	18	517	2330	7.5	86.7	1460
CM-157 + 10 nM TH-chrysenediol	61	2570	76.0	66.09	1176	1458	30.4	121	1284
CM-157 + 100 nM TH-chrysenediol	67	837	>9000	89	—	910	46.3	61	375

RU, relative unit.
[a] R_T is the total amount of dimers; it should be roughly equivalent to $B_{max}/2$. Unlike in radioligand binding studies, the B_{max} parameter does not indicate the actual level of binding sites, but it may be used for comparative purposes.

dimer (K_1 and K_2) were not significantly different. With all data-fitting protocols, the presence of 100 nM TH-chrysenediol led to a reduction in the amount of receptors. Interestingly, it was not possible to fit the data to the two independent sites, meaning that the 100 nM concentration abrogated the high-affinity binding (also noted in the similar K_1 and K_2 values under the dimer assumption). In summary, the most likely interpretation of both competition and saturation binding data is the preferential occupancy by TH-chrysenediol of a high-affinity component, thus disclosing two differential binding species in CB_2R.

Discussion

It is well known that CB_2R pharmacology is complex. Reported data using the two commercially available radioligands, both of which are nonselective ([^{3}H]-CP55940 and [^{3}H]-WIN55212-2), are not always consistent, and the functional data also reveal contradictions related to a given ligand acting as an agonist, inverse agonist, or antagonist. A clear example is AM630, a compound that is often used as a CB_2R antagonist, even by companies providing drug discovery services, but was reported to be a protean ligand (Bolognini et al., 2012). In this scenario, the appearance of a new technique, avoiding the drawbacks of radioactive-based binding and providing higher specific binding and less standard error, should be of help, especially when the labeled compound used to mark the receptors is selective. In fact, by using competitive intelligence analysis (Rabal and Oyarzabal, 2012) and additional computational studies, we have identified the first red CB_2R ligand, a molecule suitable to perform a homogenous and nonradioactive high-affinity (K_D = 19-35 nM) binding assay to CB_2R. In addition, CM-157 is CB_2R selective because the affinity for CB_1R is $> 10\ \mu M$ (i.e., the ratio of CB_2R *versus* CB_1R agonism is > 600; Gijsen et al., 2008). Advantages of the method include a higher percentage of specific binding, less variability, elimination of the burden attributable to radioactive handling and exposure, and radioactive waste disposal. Moreover, radioligand-binding techniques have not allowed making progresses in the binding to receptors on the surface of living cells. Certainly, the advantage of the assays we propose here of performing binding to CB_2R in living cells is of note.

GPCR heteromerization challenges classic pharmacological views and data analysis and interpretation. One key issue consists of knowing how heteromer formation modifies binding of a given selective agonist to its receptor. In our conditions, coexpression of two receptors able to form heteromers led to a decrease in binding, without significant modification of the K_i values deduced from CM-157 competition assays. Lower binding has consistently been found for CB_2R-containing heteromers (namely for CB_1R-CB_2R and CB_2R-GPR55) and would agree with data reported for melatonin receptor heteromers, which regulate the melatonin effect on light sensitivity in rodent photoreceptors (Baba et al., 2013). In fact, in one of the few articles devoted to analyzing radioligand binding to receptors forming heteromers, Levoye et al. (2006) showed that coexpression of the putative melatonin receptor, GPR50, with the melatonin MT_1 receptor abolished high-affinity specific binding of ^{125}I-melatonin to MT_1 receptors by formation of GPR50-MT_1 receptor heteromers. The effect of the orphan receptor, GPR50, was selective since coexpression with the MT_2 receptor did not result in any reduction in ^{125}I-melatonin binding to these melatonin receptors, although they also form heteromeric complexes with GPR50 (Levoye et al., 2006). However, a decrease in the signal in the homogeneous binding assays reported here may be attributable to a reduction of binding sites and/or to a modification in the distance between the FRET donor and acceptor caused by the partner receptor in the dimer. Hence, heteromerization may serve to qualitatively modify the characteristics of the binding of agonists to cognate receptors.

The method here reported has been instrumental to identifying TH-chrysenediol as a novel CB_2R ligand and to detecting a qualitatively different binding profile. First, this finding should be taken into account when interpreting data using this compound; in particular, it would be good to dissect out the effects mediated by cell surface receptors from those mediated by the intracellular estrogen receptors with which the compound may also interact (Omori et al., 2005). Second, the competition curve underscores two receptor binding different affinities that, interestingly, were not observed with CM-157 itself.

Remarkably, biphasic curves were also observed with AM630. Since its discovery as a cannabinoid receptor ligand, AM630 has been commonly used for in vitro and for behavioral experiments in animal models of neurodegenerative or neuropsychiatric diseases. The aminoalkylindole AM630 was first reported as a cannabinoid receptor antagonist (Pertwee et al., 1995). Later, this compound was identified as a CB_1R and CB_2R inverse agonist (Landsman et al., 1998; Ross et al., 1999). Interestingly, Bolognini et al., (2012) showed that AM630 may act as a protean agonist. In fact, in Chinese hamster ovary cells stably expressing the human CB_2R tested

in functional assays and in binding assays using the radiolabeled agonist CP55940 or guanosine 5′-*O*-(3-[^{35}S]thio)-triphosphate, AM630 behaved as a potent inverse agonist in vehicle-preincubated cells, as a low-potency agonist in SR144528 [5-(4-chloro-3-methylphenyl)-1-[(4-methylphenyl)methyl]-*N*-[(1*S*,2*S*,4*R*)-1,3,3-trimethylbicyclo[2.2.1]hept-2-yl]-1*H*-pyrazole-3-carboxamide]-preincubated cells, or as a low-potency neutral competitive antagonist in AM630-preincubated cells (Bolognini et al., 2012). The molecular basis of such diverse actions must be related to either or both structural diversity of CB_2R and/or different coupling to the signaling machinery. The biphasic behavior observed in the competition curves obtained in this work using AM630 would suggest the occurrence of different affinity states of the receptor that, in turn, may correspond to receptor species differently coupled to G_i proteins. On comparing our competition curves using fluorophore-conjugated CM-157 and those in the report using [^{3}H]CP55940, the data in the 10 to 1000 nM range are similar (i.e., a monophasic displacement with similar K_i values is observed in the "low" affinity component of the binding). Detection of receptor forms displaying affinities in the subnanomolar range deserves further experimental effort.

Acknowledgments

The authors thank Cisbio Bioassays for technical support and labeling of CM-139 and CM-157, as well as Ainhoa Oñatibia-Astibia for technical support.

Authorship Contributions

Participated in research design: Martínez-Pinilla, Rabal, Sánchez-Arias, Lanciego, Oyarzabal, Franco.

Conducted experiments: Martínez-Pinilla, Reyes-Resina, Zamarbide, Navarro.

Contributed new reagents or analytic tools: Rabal, Sánchez-Arias, de Miguel.

Performed data analysis: Martínez-Pinilla, Rabal.

Wrote or contributed to the writing of the manuscript: Martínez-Pinilla, Rabal, Lanciego, Oyarzabal, Franco.

References

Atwood BK, Straiker A, and Mackie K (2012) CB_2: therapeutic target-in-waiting. *Prog Neuropsychopharmacol Biol Psychiatry* **38**:16–20.

Baba K, Benleulmi-Chaachoua A, Journé AS, Kamal M, Guillaume JL, Dussaud S, Gbahou F, Yettou K, Liu C, Contreras-Alcantara S, et al. (2013) Heteromeric MT1/MT2 melatonin receptors modulate photoreceptor function. *Sci Signal* **6**:ra89.

Balenga NA, Martínez-Pinilla E, Kargl J, Schröder R, Peinhaupt M, Platzer W, Bálint Z, Zamarbide M, Dopeso-Reyes I, Ricobaraza A, et al. (2014) Heteromerization of GPR55 and cannabinoid CB2 receptors modulates signaling. *Br J Pharmacol* **171**:5387–5406.

Bolognini D, Cascio MG, Parolaro D, and Pertwee RG (2012) AM630 behaves as a protean ligand at the human cannabinoid CB2 receptor. *Br J Pharmacol* **165**:2561–2574.

Buckley NE (2008) The peripheral cannabinoid receptor knockout mice: an update. *Br J Pharmacol* **153**:309–318.

Bushlin I, Gupta A, Stockton SD, Jr, Miller LK, and Devi LA (2012) Dimerization with cannabinoid receptors allosterically modulates delta opioid receptor activity during neuropathic pain. *PLoS One* **7**:e49789.

Callén L, Moreno E, Barroso-Chinea P, Moreno-Delgado D, Cortés A, Mallol J, Casadó V, Lanciego JL, Franco R, Lluis C, et al. (2012) Cannabinoid receptors CB1 and CB2 form functional heteromers in brain. *J Biol Chem* **287**:20851–20865.

Campillo NE and Páez JA (2009) Cannabinoid system in neurodegeneration: new perspectives in Alzheimer's disease. *Mini Rev Med Chem* **9**:539–559.

Carai MAM, Colombo G, Maccioni P, and Gessa GL (2006) Efficacy of rimonabant and other cannabinoid CB1 receptor antagonists in reducing food intake and body weight: preclinical and clinical data. *CNS Drug Rev* **12**:91–99.

Ellis J, Pediani JD, Canals M, Milasta S, and Milligan G (2006) Orexin-1 receptor-cannabinoid CB1 receptor heterodimerization results in both ligand-dependent and -independent coordinated alterations of receptor localization and function. *J Biol Chem* **281**:38812–38824.

Ferré S, Baler R, Bouvier M, Caron MG, Devi LA, Durroux T, Fuxe K, George SR, Javitch JA, Lohse MJ, et al. (2009) Building a new conceptual framework for receptor heteromers. *Nat Chem Biol* **5**:131–134.

Gijsen HJM, De Cleyn MAJ, Surkyn M, Verbist BMP (2008) inventors, Janssen Pharmaceutica NV, assignee. Benzimidazole cannabinoid agonists bearing a substituted heterocyclic group. Patent WO2008003665. 2008 Jan 10.

Hojo M, Sudo Y, Ando Y, Minami K, Takada M, Matsubara T, Kanaide M, Taniyama K, Sumikawa K, and Uezono Y (2008) mu-Opioid receptor forms a functional heterodimer with cannabinoid CB1 receptor: electrophysiological and FRET assay analysis. *J Pharmacol Sci* **108**:308–319.

Idris AI (2010) Cannabinoid receptors as target for treatment of osteoporosis: a tale of two therapies. *Curr Neuropharmacol* **8**:243–253.

Kon-I K, Matsumizu M, Shima A (2006) inventors, Pfizer Japan Inc., assignee. Sulfonyl benzimidazole derivatives. Patent WO2006048754. 2006 May 11.

Landsman RS, Makriyannis A, Deng H, Consroe P, Roeske WR, and Yamamura HI (1998) AM630 is an inverse agonist at the human cannabinoid CB1 receptor. *Life Sci* **62**:PL109–PL113.

Leleu-Chavain N, Desreumaux P, Chavatte P, and Millet R (2013) Therapeutical potential of CB_2 receptors in immune-related diseases. *Curr Mol Pharmacol* **6**: 183–203.

Levoye A, Dam J, Ayoub MA, Guillaume JL, Couturier C, Delagrange P, and Jockers R (2006) The orphan GPR50 receptor specifically inhibits MT1 melatonin receptor function through heterodimerization. *EMBO J* **25**:3012–3023.

Malek N, Popiolek-Barczyk K, Mika J, Przewlocka B, and Starowicz K (2015) Anandamide, acting via CB2 receptors, alleviates LPS-induced neuroinflammation in rat primary microglial cultures. *Neural Plast* **2015**:130639.

Martínez-Pinilla E, Reyes-Resina I, Oñatibia-Astibia A, Zamarbide M, Ricobaraza A, Navarro G, Moreno E, Dopeso-Reyes IG, Sierra S, Rico AJ, et al. (2014) CB1 and GPR55 receptors are co-expressed and form heteromers in rat and monkey striatum. *Exp Neurol* **261**:44–52.

Navarro G, Carriba P, Gandía J, Ciruela F, Casadó V, Cortés A, Mallol J, Canela EI, Lluis C, and Franco R (2008) Detection of heteromers formed by cannabinoid CB1, dopamine D2, and adenosine A2A G-protein-coupled receptors by combining bimolecular fluorescence complementation and bioluminescence energy transfer. *ScientificWorldJournal* **8**:1088–1097.

Omori Y, Nakamura K, Yamashita S, Matsuda H, Mizutani T, Miyamoto K, and Minegishi T (2005) Effect of follicle-stimulating hormone and estrogen on the expression of betaglycan messenger ribonucleic acid levels in cultured rat granulosa cells. *Endocrinology* **146**:3379–3386.

Pertwee R, Griffin G, Fernando S, Li X, Hill A, and Makriyannis A (1995) AM630, a competitive cannabinoid receptor antagonist. *Life Sci* **56**:1949–1955.

Przybyla JA and Watts VJ (2010) Ligand-induced regulation and localization of cannabinoid CB1 and dopamine D2L receptor heterodimers. *J Pharmacol Exp Ther* **332**:710–719.

Rabal O and Oyarzabal J (2012) Biologically relevant chemical space navigator: from patent and structure-activity relationship analysis to library acquisition and design. *J Chem Inf Model* **52**:3123–3137.

Rios C, Gomes I, and Devi LA (2006) mu Opioid and CB1 cannabinoid receptor interactions: reciprocal inhibition of receptor signaling and neuritogenesis. *Br J Pharmacol* **148**:387–395.

Ross RA, Brockie HC, Stevenson LA, Murphy VL, Templeton F, Makriyannis A, and Pertwee RG (1999) Agonist-inverse agonist characterization at CB1 and CB2 cannabinoid receptors of L759633, L759656, and AM630. *Br J Pharmacol* **126**: 665–672.

Sam AH, Salem V, and Ghatei MA (2011) Rimonabant: from RIO to ban. *J Obes* **2011**: 432607.

Savonenko AV, Melnikova T, Wang Y, Ravert H, Gao Y, Koppel J, Lee D, Pletnikova O, Cho E, Sayyida N, et al. (2015) Cannabinoid CB2 receptors in a mouse model of Aβ amyloidosis: immunohistochemical analysis and suitability as a PET biomarker of neuroinflammation. *PLoS One* **10**:e0129618.

Sun YX, Xu AH, Yang Y, Zhang JX, and Yu AW (2015) Activation of cannabinoid receptor 2 enhances osteogenic differentiation of bone marrow derived mesenchymal stem cells. *BioMed Res Int* **2015**:874982.

Tao Q, McAllister SD, Andreassi J, Nowell KW, Cabral GA, Hurst DP, Bachtel K, Ekman MC, Reggio PH, and Abood ME (1999) Role of a conserved lysine residue in the peripheral cannabinoid receptor (CB2): evidence for subtype specificity. *Mol Pharmacol* **55**:605–613.

Zhang RX, Ren K, and Dubner R (2013) Osteoarthritis pain mechanisms: basic studies in animal models. *Osteoarthritis Cartilage* **21**:1308–1315.

Address correspondence to: Eva Martínez-Pinilla, Instituto de Neurociencias del Principado de Asturias, Departamento de Morfología y Biología Celular, Universidad de Oviedo, Julián Clavería s/n, 33006 Asturias, Spain. E-mail: martinezpinillaeva@gmail.com; Rafael Franco, Institute of Biomedicine, University of Barcelona, Diagonal 643, 08028 Barcelona, Spain. E-mail: rfranco@ub.edu; or Julen Oyarzabal, Small Molecule Discovery Platform, Molecular Therapeutics Program, Centre for Applied Medical Research, University of Navarra, 31008 Pamplona, Spain. E-mail: julenoyarzabal@unav.es